

The Mitochondrial Myopathy, Encephalopathy, Lactic Acidosis, and Stroke-like Episode Syndrome-associated Human Mitochondrial tRNA^{Leu(UUR)} Mutation Causes Aminoacylation Deficiency and Concomitant Reduced Association of mRNA with Ribosomes*

Received for publication, October 28, 1999, and in revised form, March 29, 2000
Published, JBC Papers in Press, April 14, 2000, DOI 10.1074/jbc.M908734199

Anne Chomyn‡, José Antonio Enriquez§, Vicente Micol¶, Patricio Fernandez-Silva§, and Giuseppe Attardi

From the Division of Biology, California Institute of Technology, Pasadena, California 91125

The pathogenetic mechanism of the mitochondrial tRNA^{Leu(UUR)} A3243G transition associated with the mitochondrial myopathy, encephalopathy, lactic acidosis, and stroke-like episodes (MELAS) syndrome has been investigated in transmittochondrial cell lines constructed by transfer of mutant mitochondrial DNA (mtDNA)-carrying mitochondria from three genetically unrelated MELAS patients or of isogenic wild-type mtDNA-carrying organelles into human mtDNA-less cells. An *in vivo* footprinting analysis of the mtDNA segment within the tRNA^{Leu(UUR)} gene that binds the transcription termination factor failed to reveal any difference in occupancy of sites or qualitative interaction with the protein between mutant and wild-type mtDNAs. Cell lines nearly homoplasmic for the mutation exhibited a strong (70–75%) reduction in the level of aminoacylated tRNA^{Leu(UUR)} and a decrease in mitochondrial protein synthesis rate. The latter, however, did not show any significant correlation between synthesis defect of the individual polypeptides and number or proportion of UUR codons in their mRNAs, suggesting that another step, other than elongation, may be affected. Sedimentation analysis in sucrose gradient showed a reduction in size of the mitochondrial polysomes, while the distribution of the two rRNA components and of the mRNAs revealed decreased association of mRNA with ribosomes and, in the most affected cell line, pronounced degradation of the mRNA associated with slowly sedimenting structures. Therefore, several lines of evidence indicate that the protein synthesis defect in A3243G MELAS mutation-carrying cells is mainly due to a reduced association of mRNA with ribosomes, possibly as a consequence of the tRNA^{Leu(UUR)} aminoacylation defect.

human mitochondrial DNA (mtDNA).¹ Investigations of their pathogenetic mechanisms can provide important information on mitochondrial protein synthesis and other aspects of mitochondrial biogenesis. Among such studies are those on the A8344G mutation in tRNA^{Lys}, which causes myoclonic epilepsy and ragged red fiber syndrome (MERRF) (2), and those on the T7445C mutation in the nucleotide immediately adjacent to the 3'-end of the tRNA^{Ser(UCN)} gene, which is associated with deafness (3, 4). The former tRNA mutation causes premature termination of translation, most likely due to a tRNA^{Lys} aminoacylation deficiency (5), while the latter mutation produces a reduction in the level of tRNA^{Ser(UCN)}, due to a defect of precursor processing, that also reduces the level of the co-transcribed ND6 mRNA (6). Protein synthesis in mitochondria with the latter mutation is presumably also affected at the level of elongation, but, rather than premature termination, there appears to be a pause in elongation, followed by a resumption of synthesis.

The pathogenetic mechanism of the most extensively investigated tRNA gene mutation, the A3243G transition in the tRNA^{Leu(UUR)} gene, which causes the MELAS encephalomyopathy (7), maternally inherited diabetes (8), or chronic progressive external ophthalmoplegia (9), is still unresolved, despite the numerous investigations on this topic. The mutation occurs in the middle of the binding site for the mitochondrial transcription termination factor, mTERF (10) (Fig. 1a). *In vitro* experiments have shown that the mutation does indeed reduce the affinity of mTERF for the DNA (11) and cause a decrease in the rate of termination of the rDNA transcription unit (12). However, an analysis of mtDNA-less human cells repopulated with mitochondria from MELAS patients (11, 13) did not reveal any significant difference from the controls in the relative steady-state levels of the two rRNA species, encoded upstream of the termination site, and of the mRNAs encoded downstream. On the other hand, the mitochondrial protein synthesis rate has been found to be decreased, as was the respiration rate, in cell lines carrying the mutation (11, 13).

The protein synthesis defect has been proposed to be due to stalling of translation by pseudoribosomes that have incorporated RNA 19, an incompletely processed transcript reported to accumulate in A3243 mutant cells, in place of 16 S rRNA (14), or possibly to defective posttranscriptional modification of the tRNA^{Leu(UUR)} (15, 16). Yet others suggest that the mutant

Mutations in tRNA genes constitute a large proportion, ~75% (1), of the disease-causing mutations identified so far in

* This work was supported by National Institutes of Health Grant GM-11726 (to G. A.). The costs of publication of this article were defrayed in part by the payment of page charges. This article must therefore be hereby marked "advertisement" in accordance with 18 U.S.C. Section 1734 solely to indicate this fact.

‡ To whom correspondence should be addressed. Tel.: 626-395-4958; Fax: 626-449-0756; chomyn@seqxp.bio.caltech.edu.

§ Present address: Dept. de Bioquímica y Biología Molecular y Celular, Universidad de Zaragoza, Miguel Servet, 177, 50013 Zaragoza, Spain.

¶ Present address: Centro de Biología Molecular y Celular, Universidad Miguel Hernández, C/Monóvar s/n (Pol. Ind. Carrús) E-03206 Elche (Alicante), Spain.

¹ The abbreviations used are: mtDNA, mitochondrial DNA; MELAS, mitochondrial myopathy, encephalopathy, lactic acidosis, and stroke-like episodes; mTERF, mitochondrial termination factor; MERRF, myoclonic epilepsy and ragged red fibers; DMS, dimethyl sulfate; L strand, light strand; H strand, heavy strand.

tRNA may cause mistranslation, leading to accelerated turnover of mitochondrial translation products (17, 18).

The results described in the present work do not fit a model in which, in MELAS mutation-carrying cells, mitochondrial translation is affected mainly at the level of elongation, either prematurely terminating at or near UUR codons or pausing at UUR codons and then resuming elongation. On the contrary, they give strong support to a model in which the A3243G mutation affects both the steady state level and the aminoacylation efficiency of the tRNA^{Leu(UUR)} and, possibly as a consequence of these changes, reduces the rate of assembly of mRNA with ribosomes, with a resulting decrease in mitochondrial translation rate.

EXPERIMENTAL PROCEDURES

Cell Culture—The cell lines used for these studies have been described previously (11, 19, 20). 143B.TK⁻ is a human osteosarcoma-derived cell line (ATCC CRL 8303); the 94I, 43B, 2SA, 2SC, 4H1, and pT1 cell lines are mitochondrial transformants of an mtDNA-less (ρ^0) derivative of 143B.TK⁻, *i.e.* ρ^0 206 (21). The cell line pT1 is a ρ^0 206 transformant that carries the A8344G MERRF mutation in the mitochondrial tRNA^{Lys} gene in nearly 100% of its mtDNA (19). 143B.TK⁻ cells and HeLa S3 cells in suspension were grown as described previously (21, 22). ρ^0 cell transformants were grown in Dulbecco's modified Eagle's medium supplemented with 10% fetal bovine serum.

DNA Sequencing—For sequencing the tRNA^{Leu(UUR)} gene, the mtDNA fragment between positions 3206 and 3728 was amplified, using 20-nucleotide-long primers, by the polymerase chain reaction. The product was then purified from an agarose gel and sequenced with a primer corresponding to heavy (H)-strand nucleotides 3511–3491. Similarly, the fragment of mtDNA between positions 11836 and 12553 that contains the tRNA^{Leu(CUN)} gene was amplified and then sequenced with light (L)-strand primer L12080–12099 or H-strand primer H12500–12479.

Determination of mtDNA Level—Total cellular DNA on slot blots was hybridized with a 498-nucleotide probe for nuclear ribosomal DNA, stripped, and then rehybridized with a 2537-nucleotide probe for mitochondrial ribosomal DNA as described (20).

In Vivo Footprinting of mtDNA—This was done as described previously (22, 23). Briefly, intact cells were treated with dimethyl sulfate (DMS), which methylates unprotected guanines and adenines (24). Total nucleic acids were then extracted and incubated with piperidine, which cleaves the DNA preferentially at the methylated guanine residues (24). The DNA was subjected to multiple rounds of primer extension from a ³²P-5'-end-labeled H strand primer, as described previously (23), and the final products were resolved on a sequencing gel.

Isolation of tRNAs and Quantification of in Vivo Aminoacylation—Highly purified total mitochondrial tRNA was isolated as described (25). Quantification of the steady state levels of individual mitochondrial tRNA species was done by RNA gel blot analysis as described (5), using ³²P-5'-end-labeled oligonucleotides specific for tRNA^{Leu(UUR)}, tRNA^{Lys}, tRNA^{Ser(UCN)}, tRNA^{Glu}, and 12 S rRNA, as detailed previously (6).

For quantification of the extent of aminoacylation of the tRNAs, a rapid procedure for isolation of the mitochondrial fraction was used. The tRNAs were extracted under acid conditions and then run on an acid-urea 6.5% polyacrylamide gel to separate the charged and uncharged tRNAs (5, 26). Quantification of band intensities was done by PhosphorImager (Molecular Dynamics, Inc., Sunnyvale, CA) analysis.

Analysis of Mitochondrial Protein Synthesis Rates—mtDNA-encoded proteins were labeled in 143B.TK⁻ and 43B cells *in vivo* for 30 min with [³⁵S]methionine in methionine-free medium in the presence of emetine, as described previously, and the labeled protein gel patterns have been published (11). For the present work, the mtDNA-encoded proteins in 2SA and 2SC cells were labeled for 20 or 40 min in the same manner, using [³⁵S]methionine (1175 Ci/mmol; Expre³⁵S³⁵S, NEN Life Science Products) at 150 μ Ci/ml in Dulbecco's modified Eagle's medium minus methionine, supplemented with 5% dialyzed fetal bovine serum. Lysates of the labeled cells were analyzed by SDS-polyacrylamide gel electrophoresis as described (27). The quantification of band intensities was done by NIH Image analysis of optical gel scans of appropriately exposed films.

To examine the stability of proteins synthesized in mitochondria, a "pulse-chase" labeling protocol was used. 94I and 43B were exposed for 2 h to 0.2 mCi/ml of [³⁵S]methionine in Dulbecco's modified Eagle's medium minus methionine, supplemented with 10% dialyzed fetal bo-

vine serum and 100 μ g/ml cycloheximide. The labeling medium was then replaced with complete, nonradioactive medium, and the cells were grown for 16 h at 37 °C before harvesting. For reference, other samples were labeled for 2 h with [³⁵S]methionine in the presence of cycloheximide and then immediately harvested.

Analysis of Mitochondrial Ribosomes and Polysomes—For the analysis of mitochondrial polysomes, cells were labeled with [³⁵S]methionine as described (5) and mixed with 143B.TK⁻ cells that had been labeled for 1 day with [5-³H]uridine in the absence of inhibitors (to provide size markers for the sucrose gradients, as described below). The mitochondrial fraction was then isolated and lysed with 2% Triton X-100 as described (28) but in the presence of 5 mM dithiothreitol and 50 units/ml RNasin (Promega). The mitochondrial lysate was run on a 15–30% sucrose gradient (28) in 100 mM Tris-HCl, pH 6.7 (25 °C), 100 mM KCl, 10 mM MgCl₂ (TKM buffer) in a Beckman SW41 rotor at 32,600 rpm for 190 min at 2 °C. Approximately 0.3-ml fractions from the gradients were collected into tubes containing 10 μ l of 2 mM dithiothreitol and 1 unit of RNasin (Promega), and a portion precipitated with 10% trichloroacetic acid in the presence of 50 μ g of bovine serum albumin. The precipitates were collected on Millipore HAWP filters, and the radioactivity was counted. In a control experiment using puromycin, the cells were incubated with 150 μ g/ml puromycin (Sigma) for 10 min immediately following the 5-min [³⁵S]methionine labeling pulse.

For the analysis of ribosomes and ribosomal subunits (28), cells were treated for 20 min with 0.1 μ g/ml actinomycin D to inhibit nuclear RNA synthesis and then labeled for 1 h (unless otherwise stated) with 0.05 mCi/ml [5-³H]uridine (22 Ci/mmol; NEN Life Science Products) in the continued presence of actinomycin D and pooled with ~10 times as many unlabeled cells and with cells labeled with [2-¹⁴C]uridine in the absence of inhibitors (see below). The mitochondrial fraction was then isolated, lysed with 2% Triton X-100, and analyzed in the sucrose gradient described above by running it in the SW41 rotor at 28,000 rpm for 13.8 h at 2 °C.

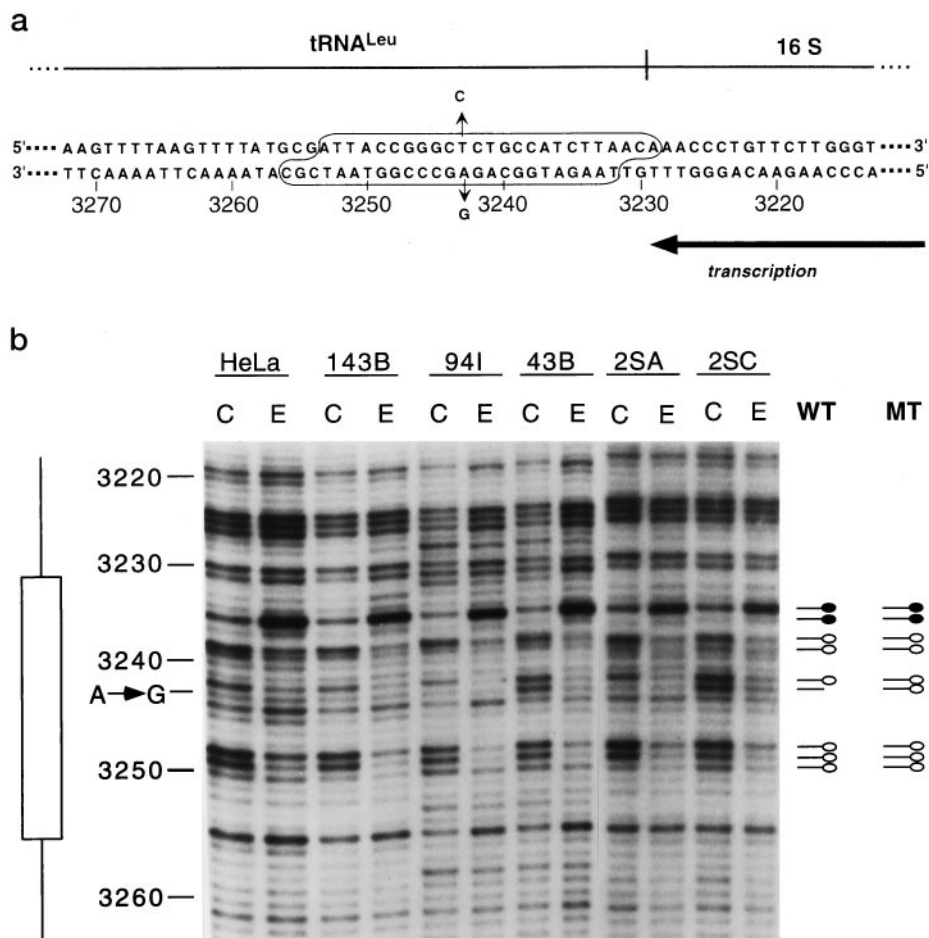
As mentioned above, size markers for the sucrose gradients were provided by the addition of [5-³H]uridine- or [2-¹⁴C]uridine-labeled 143B.TK⁻ cells to the cells that had been labeled for polysome or ribosome analysis, respectively. In particular, 2.5×10^5 cells were labeled for 1 day with 0.25 μ Ci/ml of [5-³H]uridine or of [2-¹⁴C]uridine (60 mCi/mmol; ICN) in the absence of inhibitors. Under such labeling conditions, the stable nucleus-encoded large and small subunit rRNAs incorporate most of the radioactivity. Because the cytosolic ribosomes and ribosomal subunits, with sedimentation constants 74, 60, and 40 S, always contaminate the mitochondrial fraction, they are detectable in the sucrose gradient profiles of the mitochondrial lysates by virtue of their containing the long term ³H- or ¹⁴C-labeled nucleus-encoded rRNAs.

For analysis of the RNAs in the various fractions of a sucrose gradient, pairs or triplets of fractions were pooled, and then 2 volumes of 50 mM Tris-HCl, pH 7.4, 0.3 M NaCl, 8 mM EDTA, 1% SDS, 150 μ g/ml proteinase K, and 10 μ g/ml tRNA were added. The mixtures were incubated at 37 °C for 30 min and then extracted twice with a 25:24:1 mixture of phenol/chloroform/isoamyl alcohol equilibrated with 10 mM Tris-HCl, pH 7.4, 100 mM NaCl, 1 mM EDTA, 0.5% SDS, precipitated with ethanol, and finally dissolved in 10 mM Tris-HCl, pH 7.4, 1 mM EDTA.

RNA Solution Hybridization Analysis—The RNAs from the desired fractions were pooled and divided into five equal parts. An excess of unlabeled DNA probe or mixture of probes was hybridized to each aliquot of labeled RNA in 0.4 M NaCl, 10 mM Tris-HCl, pH 7.4, 1 mM EDTA for 15 h at 60 °C. After digestion with RNases T₁ (50 units/ml) and A (40 μ g/ml), the RNase-resistant radioactivity was determined as described (29). The probes were as follows: for the detection of 16 S rRNA, 12 S rRNA, and ND1 RNA, plasmid clones containing 805 nucleotide pairs of the 16 S rRNA gene, 800 nucleotide pairs of the 12 S rRNA gene, and 809 nucleotide pairs of the ND1 gene, respectively, were used. To probe the RNAs downstream of the ND1 gene, an equimolar mixture of clones containing sequences of the COI, COII, ATPase 8/ATPase 6, COIII, ND3, ND4L/ND4, ND5, and cytochrome b genes, spanning 7424 nucleotide pairs of mRNA coding region was used. The latter set of plasmid clones contained also the sequences of tRNAs specific for Ser (both tRNAs), Asp, Lys, Glu, Arg, His, and Leu(CUN).

RNA Transfer Hybridization Analysis—This was done substantially as described previously (11). The probes for ND1 mRNA, 16 S rRNA, and 12 S rRNA were plasmids carrying the human mtDNA sequences from position 2953 to 3311, from 1768 to 2573, and from 764 to 1466, respectively. The probes for ND2 and COI mRNAs were plasmid inserts that corresponded to the human mtDNA sequence from position 4431 to 5274, and from 6203 to 6910, respectively. All were labeled with

FIG. 1. Effects of the A3243G mutation on the *in vivo* footprinting pattern of the mitochondrial rDNA transcription termination region. *a*, the portion of the human mtDNA sequence that interacts with mTERF is indicated. The A3243G mutation that causes MELAS and other diseases is also shown. *b*, footprint autoradiograms showing the methylation interference pattern produced *in vivo* in the light strand mtDNA sequence by the bound protein. *C*, control, *i.e.* DNA purified from cells before modification with DMS and cleavage with piperidine. *E*, experimental (*i.e.* modified DNA extracted from intact cells exposed to DMS and then treated with piperidine). *WT*, wild type; *MT*, mutant. The filled circles indicate sites that are hypermethylated because of the bound protein. The open circles indicate sites that are protected from modification by the bound protein. The tick with no circle indicates the A at position 3243.



[α -³²P]dCTP or [α -³²P]dATP by the random primer method (30).

Mathematical Analysis—Nonlinear curve fitting was done using the Levenberg-Marquardt algorithm (KaleidaGraph software, Synergy).

RESULTS

Cell Lines—The cell lines 43B and 2SC, which carried the A3243G mutation in nearly homoplasmic form (99 and 97%, respectively) had been previously shown to have decreased mitochondrial protein synthesis rates (~20 and ~50%, respectively, of the wild-type rates, after a 30-min labeling pulse with [³⁵S]methionine) and markedly reduced respiration rates (<10 and ~18%, respectively, of the wild-type rates) (11). Another mutant cell line, 4H1, that carried 98% mutant mtDNA (20), was used in some of the analyses presented here. The 143B.TK⁻ cell line, and transmittochondrial cell lines 94I and 2SA all exhibited 100% wild-type DNA at position 3243 (11). Cell lines 94I and 43B are isogenic except at position 3243, as are the pair 2SA and 2SC.

The sequences of the tRNA^{Leu(UUR)} genes in 94I and 43B had been previously shown (15) to be identical to the Cambridge sequence (31) outside of position 3243. Polymerase chain reaction amplification and sequencing of the tRNA^{Leu(UUR)} gene from the 2SC and 4H1 cell lines (this work) also failed to reveal any difference from the standard sequence. Furthermore, in order to investigate the possible presence in the mutant cells of a suppressor mutation in the other mitochondrial tRNA^{Leu} gene, like the one at position 12,300 that has been recently reported (32), the mitochondrial tRNA^{Leu(CUN)} gene of the 43B, 4H1, 2SA, and 2SC cell lines was polymerase chain reaction-amplified and sequenced. No mutation at position 12,300 or at any other position was found in this gene in any of the cell lines.

The amount of mtDNA relative to nuclear DNA in the cell

lines 94I, 43B, 2SA, 2SC, and 4H1 was 129, 103, 130, 100, and 83%, respectively, of that in 143B.TK⁻ cells.

In Vivo Footprinting of mTERF mtDNA Binding Site—Previous evidence from *in vitro* experiments had shown that the A3243G mutation decreased the binding of mTERF to mtDNA and the efficiency of transcription termination (11, 12). In view of the discrepancy of these results with the observed lack of any effect of the mutation on the ratio of transcripts downstream to those upstream of the termination site (11, 13), in the present work *in vivo* footprinting experiments were carried out to determine whether the A3243G mutation reduces the occupancy of the mTERF binding sites or causes changes in the methylation interference pattern in living cells.

Fig. 1*b* shows the *in vivo* footprint of the mtDNA L strand of the rDNA transcription termination region for several cell lines that are wild-type at position 3243, namely HeLa, 143B.TK⁻, 94I, and 2SA, and two cell lines that carry the A3243G transition (in ≥97% of their mitochondrial genomes), 43B and 2SC. The footprints of the protein can be seen in the lanes marked E between positions 3232 and 3256, in agreement with data from *in vitro* DNase I protection experiments (10) and from previously reported *in vivo* footprinting experiments (22). The region protected from modification by DMS is the same in wild-type and mutant cells. An analysis of the patterns from mutant cells, after normalization to reference bands outside the mTERF binding site, reveals protection of the new G residue at position 3243. As the adjacent G at position 3242 is protected in both wild-type and mutant cells, it is likely that protein protects position 3243 in control cells as well as in mutant cells, but this effect is not detected because methylated A is not efficiently cleaved by piperidine (24). The G at position 3244 is affected in its *in vivo* methylation pattern, but inconsistently; it

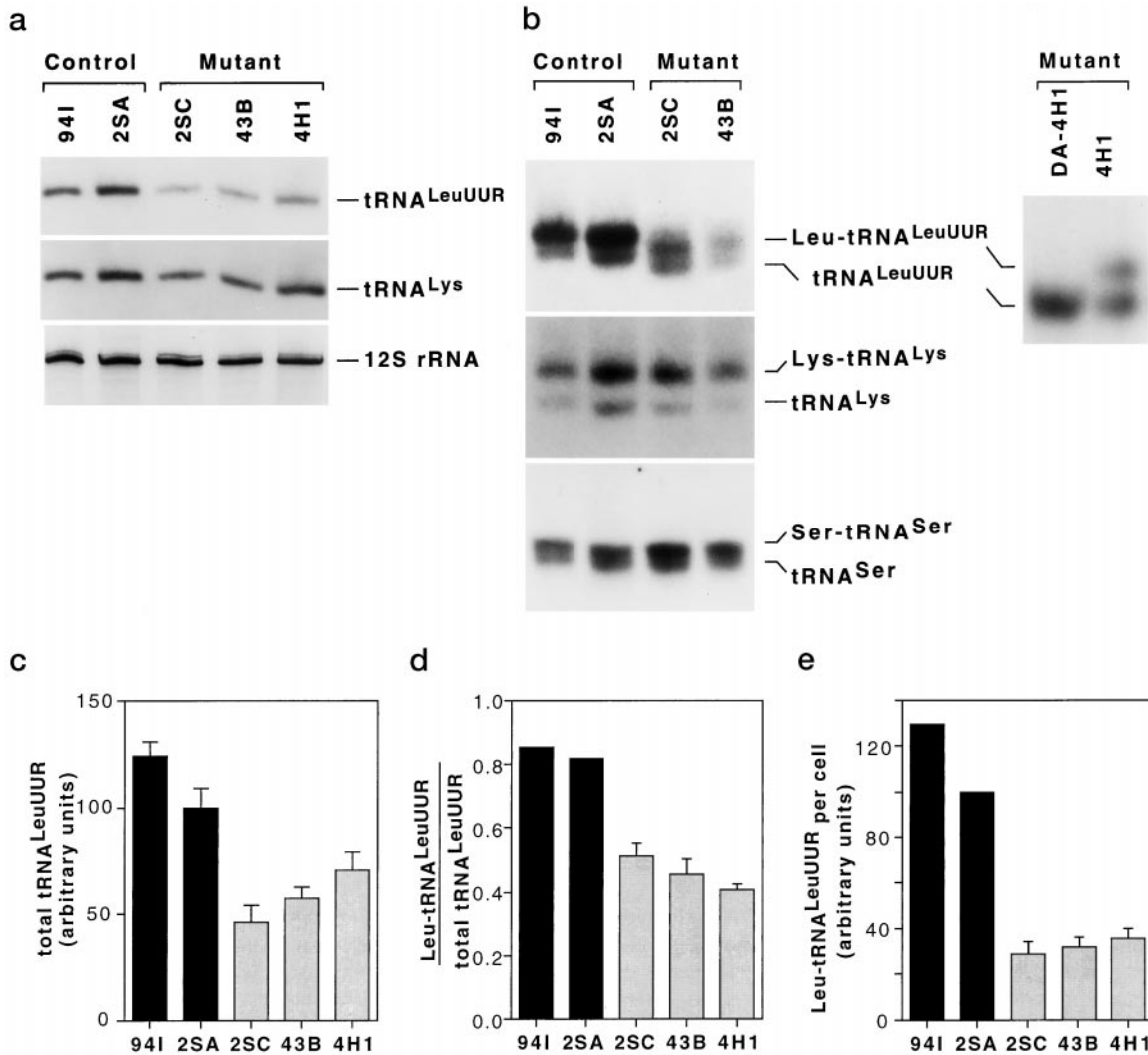


FIG. 2. RNA transfer hybridization analysis of tRNAs isolated from 94I and 2SA control cells and 43B, 2SC, and 4H1 mutant cells. *a*, the total mitochondrial tRNAs from the indicated sources were fractionated on a polyacrylamide gel, transferred onto a ZetaProbe nylon membrane (Bio-Rad), and hybridized successively with the indicated three specific probes. *b*, *left panel*, the total tRNA from the indicated sources was isolated under conditions that preserved the amino acid-tRNA bond, fractionated on an acid-urea gel, transferred onto nylon membranes, and hybridized successively with the indicated specific probes. *b*, *right panel*, samples of total tRNA from 4H1 cells, isolated as described above, were electrophoresed either untreated or after deacylation by exposure to 65 °C at pH 8 for 10 min (DA) and then blotted and hybridized with the probe for tRNA^{Leu(UUR)}. *c*, total amount of tRNA^{Leu(UUR)} per cell; *d*, proportion *in vivo* of the aminoacylated tRNA^{Leu(UUR)}; *e*, amount per cell of charged tRNA^{Leu(UUR)} in control cell lines 94I and 2SA and in mutant cell lines 2SC, 43B, and 4H1. Error bars represent one S.E.

is hypermethylated in 143B.TK⁻ and HeLa cells, in agreement with published data (22), and also in 94I cells. By contrast, this G is protected in 43B mutant cells. However, the modification of methylation of this G is marginal in 2SA and 2SC cells. It is not clear whether any significance is to be attributed to this variable base modification.

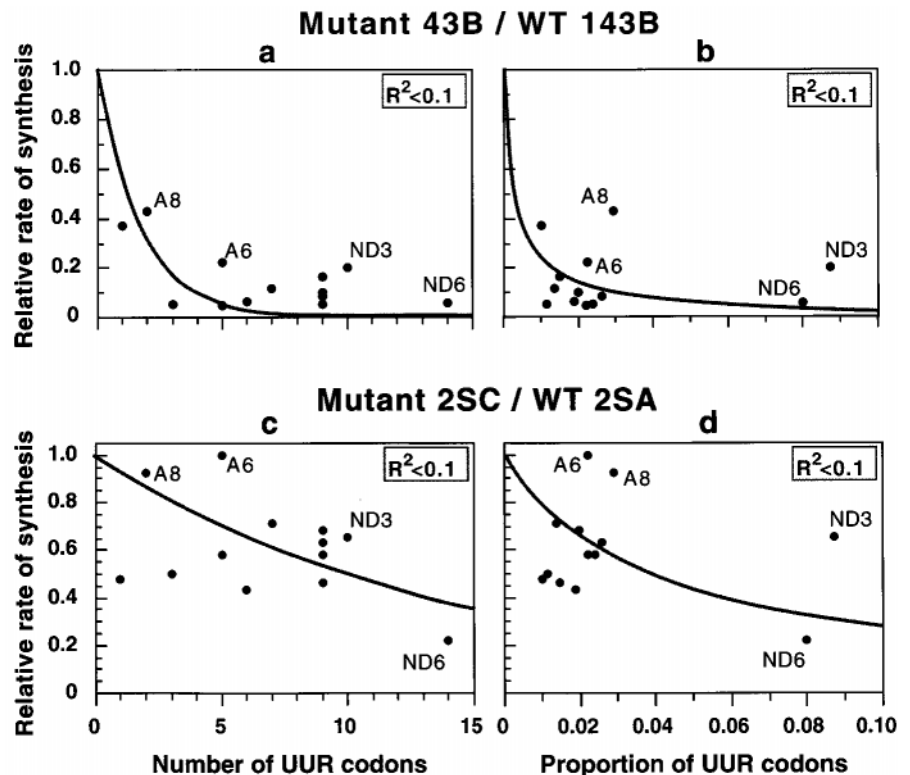
Apart from the differences at 3243 and, possibly, at 3244, there are no significant qualitative differences in the methylation interference pattern of the mitochondrial rDNA termination region between the mutants 43B and 2SC, on one hand, and their isogenic controls, 94I and 2SA, respectively, or the parental cell line 143B.TK⁻, on the other. Furthermore, a densitometric analysis showed that, after correction for loading differences, there is no significant consistent quantitative change between mutant and control patterns in the nucleotide protection or hypermethylation within the mTERF binding segment in the tRNA^{Leu(UUR)} gene.

Amount and Specific Aminoacylation of Mutant tRNA^{Leu(UUR)}—The transfer hybridization analysis of mitochondrial tRNAs in Fig. 2*a* shows that there is no obvious difference in electrophoretic mobility between the mutant

tRNA and the wild-type species (compare, for example, 2SA and 2SC). Correct processing of the mutant tRNA^{Leu(UUR)} from its precursor had previously been shown by a structural analysis of the 5'- and 3'-ends of mutant and wild-type tRNA^{Leu(UUR)} (33) and confirmed recently by direct analysis of the nucleotide composition (including modified nucleotides) of the radioactively pure tRNA (15). On the other hand, the steady state amount of tRNA^{Leu(UUR)}, when normalized to the values for tRNA^{Lys}, tRNA^{Ser}, tRNA^{Glu}, and 12 S rRNA, appears to be reduced in 43B to 47, 35, 42, and 60%, respectively (mean 46%), of the isogenic control, 94I; in 2SC to 41, 32, 42, and 69% (mean 46%) of the isogenic control, 2SA; and in 4H1 to 63, 55, 46, and 86% of the control average (mean 62%) (Fig. 2*c*).

The proportion of tRNA that is charged with amino acid *in vivo* was determined for several mitochondrial tRNAs (Fig. 2*b*), using acid conditions for RNA extraction and gel electrophoresis (26). The cell lines carrying the A3243G mutation showed a specific marked reduction in the efficiency of charging of tRNA^{Leu(UUR)}, which was only 46% in 43B, as compared with 85% in 94I, 51% in 2SC, as compared with 82% in 2SA, and 41% in 4H1 (Fig. 2*d*). By contrast, the tRNA^{Lys}, transcribed

FIG. 3. Relationship between relative rate of synthesis of the individual mitochondrial translation products and UUR content of their mRNAs in mutant cells. The rates of labeling of individual mtDNA-encoded polypeptides in 43B (*a* and *b*) or 2SC (*c* and *d*) mutant cells, after a 30- (*a* and *b*) and 40-min (*c* and *d*) pulse with [³⁵S]methionine, expressed relative to the corresponding control rates in 143B.TK⁻ or 2SA cells, are plotted against the number of UUR codons in the corresponding reading frames (*a* and *c*) or against the proportion of the UUR codons of the reading frames (*b* and *d*). The best fitting curves defined by equations for a premature termination model (*a* and *c*) or a transient pause model (*b* and *d*) are drawn in gray. R^2 , the coefficient of determination, is a measure of how well the data fit the curve. WT, wild-type.



from the H strand, like *tRNA^{Leu(UUR)}*, and the *tRNA^{Ser(UCN)}*, transcribed from the L strand, were charged at normal levels in the A3243G mutant cells (Fig. 2*b*). By combining the decrease in the amount per cell of total *tRNA^{Leu(UUR)}* and the reduction in the efficiency of aminoacylation of this *tRNA* in mutant cells, the absolute levels of total aminoacylated *tRNA^{Leu(UUR)}* per cell in the different cell lines were calculated to be, in 43B and 2SC, only 25 and 29%, respectively, relative to the levels found in the corresponding control cell lines 94I and 2SA, and in 4H1 the level was found to be 31% of the average level in the controls (Fig. 2*e*).

Testing of Models of Elongation Defect in Mitochondrial Protein Synthesis in Mutant Cells—Previous work (11) had shown that 43B cells exhibited, after a 30-min [³⁵S]methionine pulse, an ~80% decrease in the average rate of labeling of the various mtDNA-encoded polypeptides, relative to their average rate of labeling in the control cell lines. In Fig. 3*a*, the 30-min labeling data for the individual polypeptides in 43B relative to the values for 143B.TK⁻ are plotted *versus* the number of leucine (UUR) codons and tested for fit to a model according to which each leucine (UUR) codon reduces by a certain percentage the probability of elongation continuing at that site. The equation describing this “premature termination” model, previously proposed for the *tRNA^{Lys}* A8344G mutation associated with the MERRF syndrome (5), is of the form $y = y_0 \cdot A^n$, where y is the rate of synthesis of a given polypeptide in the mutant cells relative to its synthesis rate in wild-type cells, y_0 is the theoretical relative rate of polypeptide synthesis for a reading frame that has no UUR codons, A is the average probability that chain elongation continues at each UUR codon, and n is the number of UUR codons in the reading frame. It should be noted that, in the above equation, the rate of synthesis, y , refers to rate of production of a completed polypeptide chain, not to elongation rate. If the premature termination defect were to fully explain the decrease in synthesis rates, y_0 would be equal to 1.0. A curve-fitting algorithm was applied, setting y_0 at 1.0 and optimizing the value for A . As shown in Fig. 3*a*, the best curve for the 43B protein synthesis data exhibits a rather poor

fit, the coefficient of determination, R^2 , being < 0.10 . In agreement with the conclusion that the relative labeling data of the individual polypeptides in 43B cells do not fit a model of premature termination of translation, no truncated polypeptides, as were found in MERRF mutation-carrying cells (5), or labeled bands corresponding to possible peptidyl-tRNAs were observed in the patterns of newly synthesized mitochondrial translation products.

The labeling data of the mitochondrial translation products in 43B cells, relative to those for 143B.TK⁻, when plotted *versus* the *proportion* of UUR codons in the reading frames, also do not appear to fit an alternative model, the “transient pause” model, according to which the ribosome stalls at each UUR codon for a certain time and then resumes elongation in the proper frame. The equation describing that model, which was previously proposed for the T7445C mutation affecting *tRNA^{Ser(UCN)}* synthesis and associated with sensorineural deafness (6), is of the form $y = y_0 / ((1 - x) + df \cdot x)$, where x is the proportion of codons in a reading frame that are UUR, and df is the delay factor, *i.e.* the elongation time at a UUR codon divided by the average elongation time at all the other codons. If we set y_0 to 1.0, assuming that only the transient pause at UUR codons determines the decrease in protein synthesis rates, and we optimize the value for df , the equation describing this model that best conforms to the data defines also a very poorly fitting curve ($R^2 < 0.10$) (Fig. 3*b*). Subsequently, an analysis of the relative rate of synthesis of the various polypeptides *versus* the number or proportion of UUR codons in 43B mutant cells relative to 94I wild-type cells confirmed the results obtained with 43B cells relative to 143B.TK⁻ wild-type cells (data not shown).

In 2SC cells, which contained ~97% mutant mtDNA (11), mitochondrial protein synthesis was somewhat less affected than in 43B cells. In particular, in these cells, the mitochondrial translation products were labeled on the average, after a 20- or 40-min [³⁵S]methionine pulse, ~20 or ~40%, respectively, less than in 2SA cells. Again, the relative labeling data for the individual polypeptides do not show any significant

correlation with either the number or proportion of UUR codons in their reading frame, which would conform, respectively, to the premature termination of translation model ($R^2 < 0.10$) or the transient pause model ($R^2 < 0.10$). This is shown in Fig. 3, *c* and *d*, for the 40-min labeling data. Very similar results were obtained for the data from a 20-min [³⁵S]methionine pulse. No abnormal [³⁵S]methionine-labeled bands representing possible truncated polypeptides or peptidyl-tRNAs were observed in the mitochondrial translation patterns from 2SC cells, even after a 20-min pulse, supporting the conclusion that no premature termination of translation occurs in these cells either.

As shown in Fig. 3, the synthesis rates of the various polypeptides differed from one another in both 43B and 2SC cells. However, these differences tended to be similar for most of the mtDNA-encoded polypeptides in the two types of cells, as appears most clearly for A6, A8, ND3, and ND6 in Fig. 3.

Stability of Newly Synthesized Mitochondrial Translation Products—A pulse-chase labeling experiment was carried out to assess the stability of the proteins synthesized in mitochondria of 43B mutant and 94I wild-type cells, with the rationale that generalized instability of the proteins from mutant cells could point to a misincorporation of amino acids resulting from the tRNA^{Leu(UUR)} mutation. The gel patterns of cells pulse-labeled for 2 h with [³⁵S]methionine in the presence of cycloheximide and then grown further in complete medium for 16 h in the absence of [³⁵S]methionine and cycloheximide were compared with the gel patterns of cells harvested immediately after a 2-h labeling pulse, correcting for differences in loading or labeling, using as reference cytosolically synthesized proteins that were labeled despite the presence of cycloheximide. The analysis revealed that the majority of the proteins synthesized in mitochondria of 43B cells (including COIII, ND1, ND2, ND3, ND4, and ND6) were as stable as those synthesized in mitochondria of 94I cells (data not shown).

Reduced Polysome Size in Mutant Cells—The data presented above on the lack of correlation between labeling rate of the individual polypeptides and the UUR codon content of their mRNAs suggested that the protein synthesis defect in cells with the A3243G tRNA^{Leu(UUR)} mutation was not of the type previously described for the tRNA^{Lys} MERRF mutation nor of that described for the T7445C mutation adjacent to the tRNA^{Ser(UCN)} gene. To gain more information on how the A3243G mutation could affect protein synthesis in a way that did not depend on the number or proportion of UUR codons, the mitochondrial polysome size distribution, after sedimentation in a sucrose gradient, was analyzed in lysates from the cell lines investigated here. To visualize the monosomes and polysomes, the nascent polypeptide chains on mitochondrial ribosomes were labeled in the two mutant (43B and 2SC) cell lines and in the two corresponding isogenic wild-type (94I and 2SA) cell lines for 5 min with [³⁵S]methionine in the presence of emetine (at a concentration previously shown to inhibit all cytosolic polysome labeling (28)). The [³⁵S]methionine-labeled cells were mixed, to provide size markers, with cells that had been long term labeled with [5-³H]uridine in the absence of inhibitors, and Triton X-100 lysates of the mitochondrial fractions were then run in sucrose gradients. As illustrated in Fig. 4*a*, all of the [5-³H]uridine profiles showed the expected three peaks corresponding to the cytosolic 74 S ribosomes and 60 and 40 S ribosomal subunits. Furthermore, all of the sucrose gradient patterns (except 94I puromycin) showed the ³⁵S-labeled mitochondrial monosomes (28) sedimenting just ahead of the cytosolic large ribosomal subunit 60 S marker and, therefore, clearly sedimenting faster than the expected position of the mitochondrial 55 S ribosomes (34). Peaks corresponding to

disomes (~80 S) and, in wild-type cell patterns, also trisomes (~105 S) were apparent as well; larger polysomes were less well separated. That these profiles did indeed represent monosomes and polysomes was demonstrated by the observation that the [³⁵S]methionine label was released from the pulse-labeled structures by puromycin (Fig. 4*a*). A comparison of the profiles from mutant cells, 43B and 2SC, with those from the respective isogenic wild-type cells (94I and 2SA) clearly revealed a change in the distribution of polysomes toward a smaller size in the mutant cells and, in 43B, a much reduced labeling of monosomes and disomes. These results indicated that the number of ribosomes per mRNA molecule was decreased in mutant cells.

Unusual mRNA-containing Structures in Mitochondria of Mutant Cells—There were two possible explanations for the observation of smaller mitochondrial polysomes in the A3243G mutation-carrying cells. The first explanation was premature translation termination and release of incomplete polypeptides or peptidyl-tRNAs at or near UUR codons. However, the absence of abnormal [³⁵S]methionine-labeled bands, even after pulses as short as 20 min, in the numerous patterns of newly synthesized mitochondrial translation products analyzed in the present work appeared to argue against this possibility. The second explanation was that the rate of loading of ribosomes onto the mRNAs was decreased in mutant cells. To investigate the latter possibility, an analysis of the distribution in a sucrose gradient of the newly assembled mitochondrial ribosomes and ribosomal subunits was carried out. For these experiments, mitochondrial RNA was labeled in different cell lines for 1 h with [5-³H]uridine in the presence of actinomycin D to inhibit nuclear RNA synthesis, and Triton X-100 lysates of the mitochondrial fractions were then run on sucrose gradients. Fig. 4*b* shows that, in the patterns from the control cell lines 94I and 2SA, the mitochondrial monosomes, migrating slightly ahead of the cytoplasmic 60 S marker, the large mitochondrial ribosomal subunit, migrating at 39 S, and the small mitochondrial ribosomal subunit, migrating at 28 S (34), were clearly separated. By contrast, in the profile from the mutant cell line 43B, the 28 S peak was unexpectedly obscured by a large peak formed by heterogeneous material centered at ~25 S. A major part of the pulse-labeled RNA in this region was very unstable, since the amount of ³H label in this peak, relative to the amount of label in the ribosomal subunits, declined markedly after 2- and 4-h pulses (Fig. 5).

The sedimentation profile of ³H-labeled RNA-containing structures in the region of the mitochondrial ribosome and ribosomal subunits derived from the mitochondrial lysate of [5-³H]uridine pulse-labeled 2SC mutant cells was also abnormal, pointing to an accumulation of heterogeneous material. In this case, however, this material was faster sedimenting, migrating between 28 and 60 S (Fig. 4*b*). This material obscured in part the 28 and 39 S peaks, as is clear by comparison with the profile from wild-type 2SA cells and the profile from MERRF tRNA^{Lys} mutation-carrying pT1 cells (Fig. 4*b*).

To identify the pulse-labeled RNA giving rise to the unusual peak in the gradient of the 43B mitochondrial lysate, solution hybridization assays using appropriate unlabeled probes were carried out on RNA phenol-extracted from the 14–33 S region of the sucrose gradient patterns from these cells and from 143B.TK⁻ wild-type cells. The results of these experiments indicated that the excess of pulse-labeled material sedimenting in the 14–33 S region of the sucrose gradient from 43B mutant cells contained mainly mRNA sequences (Fig. 6). The absence of accumulation of ³H-labeled ND1 mRNA presumably reflected the slowed processing of this RNA, evident from the presence of the processing intermediate RNA 19 (13), which is

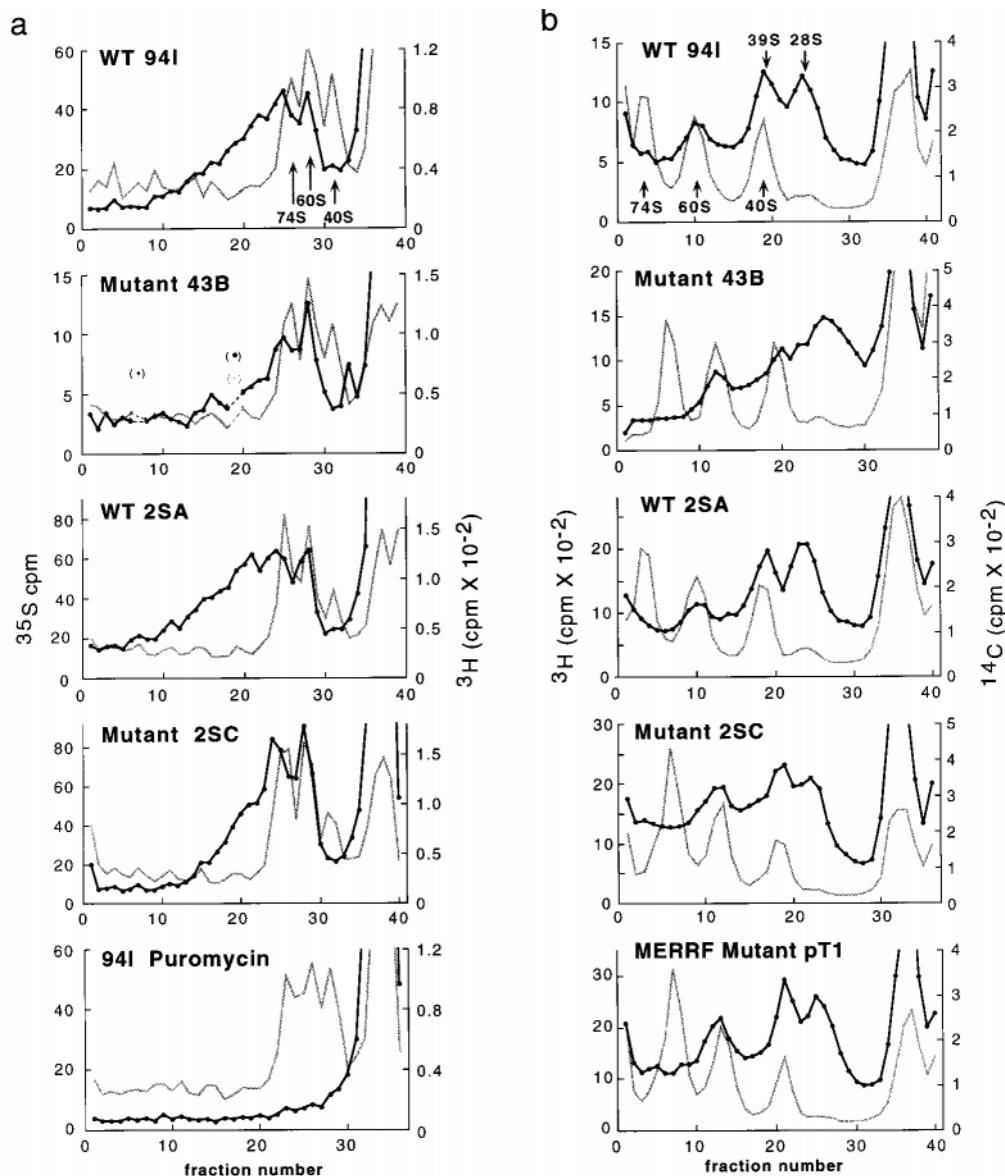


FIG. 4. Sucrose gradient profiles of mitochondrial polysomes and of ribosomes and ribosomal subunits in wild-type (WT) and mutant cells. *a*, the black lines indicate the gradient profiles of $[^{35}\text{S}]$ methionine radioactivity, derived from 5-min pulse labeling of the nascent polypeptide chains in mitochondria. The gray traces indicate the $[5\text{-}^3\text{H}]$ uridine radioactivity profiles derived from long term labeling of the cytosolic ribosomes and subunits. Note the difference in scale of the y axis for the profile for 43B mutant cells. *b*, the black lines indicate the $[5\text{-}^3\text{H}]$ uridine radioactivity profiles, derived from a 1-h pulse-labeling of mitochondrial RNA. The gray traces indicate the $[2\text{-}^{14}\text{C}]$ uridine profiles, derived from long term labeling of the cytosolic ribosomes and subunits. The bottom of each gradient is at the left.

more abundant in 43B cells than in 143B.TK⁻ cells (see below).

The experiments described above quantified newly synthesized RNAs. However, the accumulation of mRNA sequences in the 14–33 S region of the sucrose gradient from 43B cells could be confirmed by an analysis of the steady state levels of RNAs in this material isolated from a repeat experiment. Thus, in an RNA transfer hybridization analysis of fractions which spanned, as indicated in Fig. 7*a*, the portion of the sucrose gradient that included the mitochondrial ribosomal subunits, probes specific for ND1, ND2 (Fig. 7*a*), and COI mRNAs (not shown) hybridized, in addition to the full-length mRNA species, to abundant heterogeneous material, smaller than intact ND1, or ND2, or COI mRNAs, respectively. The 12 S rRNA-specific probe (Fig. 7*a*) and the 16 S rRNA-specific probe (not shown) did not detect any smear of heterogeneously sized material in the same region of the gradient. The rRNA probes did reveal, however, a few discrete degradation products; these occurred only in the same fractions that contained the full-length rRNA,

pointing to the occurrence of nicks in the isolated rRNAs. An RNA transfer hybridization analysis carried out with the corresponding gradient fractions from a mitochondrial lysate of 143B.TK⁻ wild-type cells showed very little heterogeneously sized material (Fig. 7*b*). In other experiments, an RNA transfer hybridization analysis of the sucrose gradient fractions corresponding to the mitochondrial ribosomal subunits from 94I wild-type, and 2SC and pT1 mutant cells showed a markedly lower amount of heterogeneously sized material hybridizing with ND1 or ND2 probes than was observed in the pattern from 43B cells (not shown).

The probe for ND1 mRNA also detected, in the RNA gel blots of Fig. 7, *a* and *b*, RNA 19, the previously mentioned incompletely processed H strand transcript of the 16 S rRNA, *tRNA^{Leu(UUR)}*, and *ND1* genes (13). This RNA was found in structures migrating slightly faster than the large mitochondrial ribosomal subunit. RNA 19 appeared to be more abundant in the blot from the 43B mutant cells than in that from the

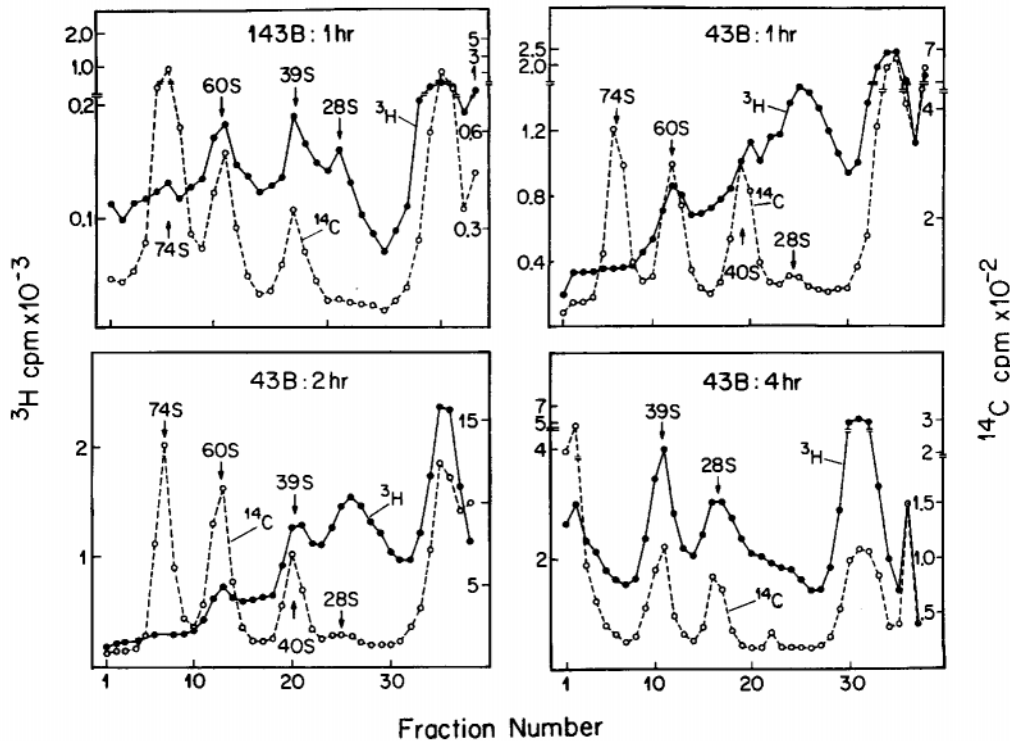


FIG. 5. **Instability of RNA in 25 S structures.** Mitochondrial RNA was labeled *in vivo* with [5-³H]uridine, in the presence of actinomycin D, in 143B.TK⁻ wild-type cells and in 43B mutant cells for the indicated times. Mitochondrial lysates were fractionated in 15–30% sucrose gradients. The gradient depicted in the lower right panel was run for 14.8 h at 32,600 rpm instead of 13.8 h at 28,000 rpm. The data in the different panels have not been normalized. Filled circles, ³H cpm; open circles, ¹⁴C cpm.

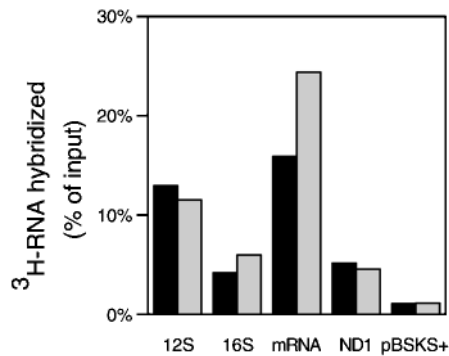


FIG. 6. **Proportion of 16 S rRNA, 12 S rRNA, mRNA, and ND1 mRNA in the 14–33 S region of the sucrose gradient after fractionation of mitochondrial lysates from 143B.TK⁻ and 43B cells.** 143B.TK⁻ wild-type and 43B mutant cells were labeled for 1 h with [5-³H]uridine, mitochondrial lysates were fractionated, RNA was extracted, and samples were hybridized in solution with DNA probes corresponding to various segments of the mitochondrial genome. Data for RNase A- and T1-resistant radioactivity are plotted. pBSKS⁺, control hybridization carried out with empty vector pBluescript KS⁺. Black bars, 143B.TK⁻ wild type; gray bars, 43B mutant.

143B.TK⁻ wild-type cells (Fig. 7b). The probe for 16 S rRNA detected RNA 19 in the identical distribution in the gradient, although RNA 19 was present in a very minor amount relative to 16 S rRNA (not shown).

Distribution of rRNAs among Submitochondrial Structures—For the determination of the distribution in the sucrose gradients of the two mitochondrial rRNA species, of the ND1 mRNA, and of RNA 19, an experiment was carried out in which the mitochondrial lysates from 94I wild-type and 43B mutant cells were fractionated in sucrose gradients, and the RNA was extracted from fractions along the entire gradient, from the pellet to the meniscus. RNA gel blot analysis was carried out on these RNA preparations with probes for 12 S rRNA, 16 S rRNA,

and ND1 RNA. The hybridization signals observed with probes for the 16 and 12 S rRNAs (blots not shown) were quantified, and the data were grouped into rRNAs associated with mitochondrial polysomes and monosomes and rRNAs associated with ribosomal subunits (Fig. 8). Also shown in Fig. 8 are data from a similar experiment in which mitochondrial lysates from 2SC MELAS mutant cells and from pT1 MERRF mutant cells were fractionated on sucrose gradients. One can see that a major portion, 56%, of the 16 and 12 S rRNA species from 94I wild-type cells migrated in the sucrose gradient with polysomes and monosomes and that 35% migrated with ribosomal subunits. By contrast, there was a clear shift in the distribution of the two rRNA species in the sucrose gradient patterns from the MELAS mutation-carrying cells, so that only 47%, in 43B, and 45%, in 2SC, of these species were associated with monosomes and polysomes, and 45 and 44%, respectively, were associated with ribosomal subunits. Also to be noted in Fig. 8 is that, in pT1 cells, which carry the MERRF tRNA^{Lys} mutation, the distribution of the rRNA species in the sucrose gradient is almost identical to that of the 94I wild-type cells. The hybridization signal of RNA 19 with the 16 S rRNA probe, relative to 16 S rRNA, was ~1% in the gradients of the mitochondrial lysates from 94I and 43B cells and ~2% in those from 2SC and pT1.

Hybridization of the same blots with an ND1 probe (data not shown), confirmed the presence of abundant degraded ND1 transcripts in the region of the sucrose gradient corresponding to ribosomal subunits in the pattern from 43B mutant cells and only minor amounts of such degraded transcripts in the region of monosomes and polysomes. The pattern from 2SC cells showed, as compared with that from control cells, a greater proportion of ND1 mRNA in the region of ribosomal subunits relative to that in the region of ribosomes and polysomes, as would be expected for reduced ribosome loading. Furthermore, we determined that the molar amount of ND1 RNA sequences

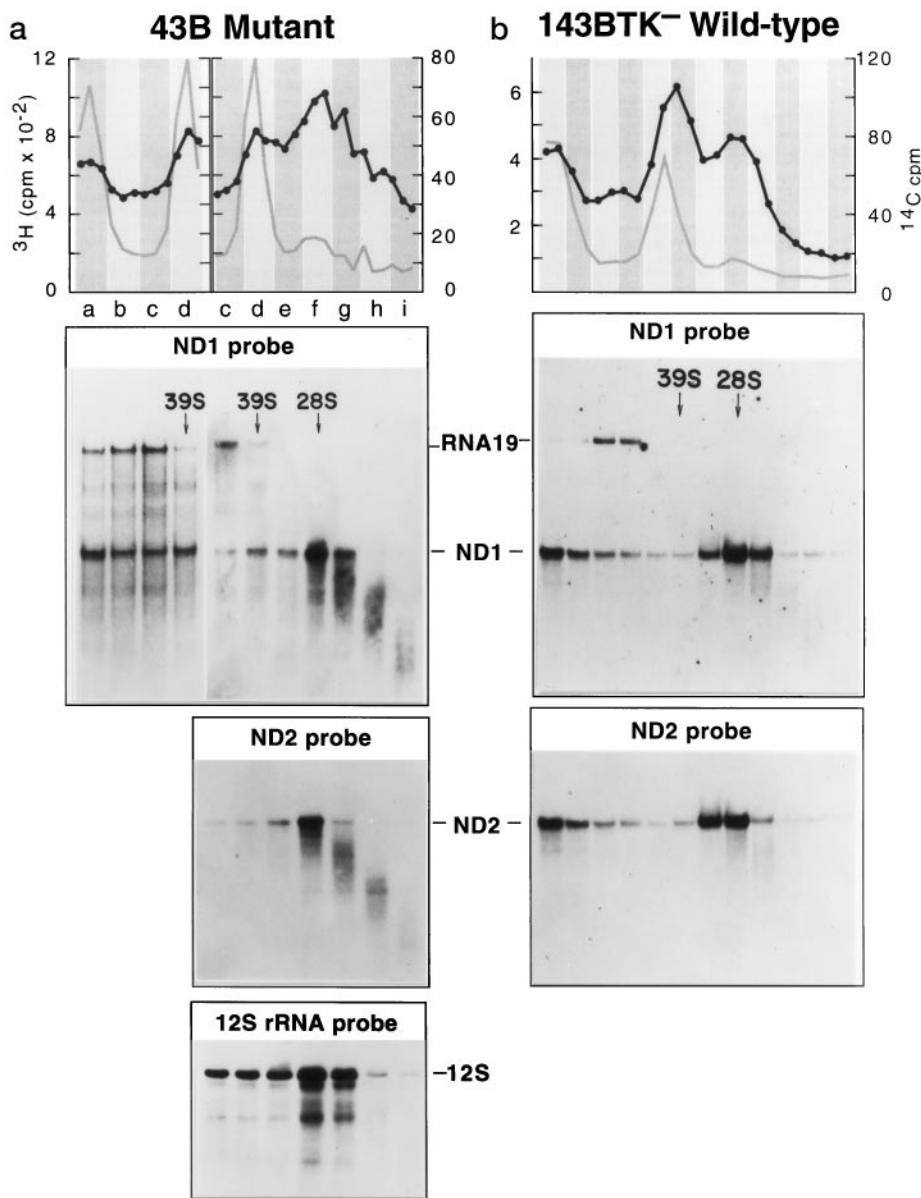


FIG. 7. RNA gel blot analysis of sucrose gradient fractions of 43B and 143B mitochondrial lysates. *a*, portions of sucrose gradient fractionation profile of a mitochondrial lysate from 43B MELAS mutant cells (*a*, upper panel) and of a lysate from 143B.TK⁻ wild-type cells (*b*, upper panel), both labeled for 1 h with [³H]uridine. The middle and lower panels show RNA transfer hybridization analysis of fractions of the gradients shown in the upper panels. Hybridization was carried out with probes for ND1 mRNA, ND2 mRNA, and 12 S rRNA. In *a*, sedimentation and hybridization patterns from two overlapping portions of the gradient are presented.

associated with RNA 19 over the whole sucrose gradient, relative to that associated with all RNA species hybridizing to the ND1 probe (*i.e.* RNA 19 and intact and degraded ND1 mRNA), was ~9% in 43B cells, as compared with 12, 12, and 10% in 94I, 2SC, and pT1 cells, respectively.

DISCUSSION

Nature of the Mitochondrial $tRNA^{Leu(UUR)}$ Defect—The decrease in level of total $tRNA^{Leu(UUR)}$ observed in the mutant cell lines (46–62% of the control values) could arise either from decreased rate of formation from the corresponding primary heavy strand transcript or from a decreased metabolic stability. Regarding the former possibility, the amount of RNA 19 (16 S + $tRNA^{Leu(UUR)}$ + ND1), which may be a precursor of $tRNA^{Leu(UUR)}$, was greater in the 43B mutant transformant than in the 143B.TK⁻ parental cell line. However, it was even greater in the 94I isogenic wild-type transformant, indicating that processing of at least this putative precursor molecule is not slowed by the mutation. Nor was there any evidence of other molecules representing abnormally processed $tRNA^{Leu(UUR)}$ in the gel electrophoresis patterns. The alternative explanation for the reduced level of $tRNA^{Leu(UUR)}$ (*i.e.* a decreased metabolic stability) is a very likely possibility. As

recognized previously (13, 15), the A3243G mutation could very well destabilize the tertiary structure of the molecule, making it more susceptible to nucleolytic attack. The A3243G mutation occurs at position 14 in the consensus structure of tRNA. The base at this position is an invariant A in bacterial and cytosolic eukaryotic tRNAs and is typically involved in the tertiary folding of classical tRNAs (35).

As concerns the explanation for the decrease in the aminoacylation efficiency of the mutant $tRNA^{Leu(UUR)}$, the A3243G MELAS mutation does not occur in one of the two regions of the tRNA structure that typically contain the identity elements, namely the acceptor stem and the anticodon (36–38). Nevertheless, the mutation may directly affect binding of the $tRNA^{Leu(UUR)}$ to the synthetase, exacerbating the probable contribution of the structural destabilization to the decrease in aminoacylation rate (39–41).

In addition, the post-transcriptional methylation of the G at nucleotide 3239 (position 10 in the consensus tRNA structure) has been found to be reduced by 50% in 43B mutant cells relative to 94I isogenic wild-type cells (15), and a deficiency of the secondary modification of the uridine at the first position of the anticodon has recently been reported in other A3243G

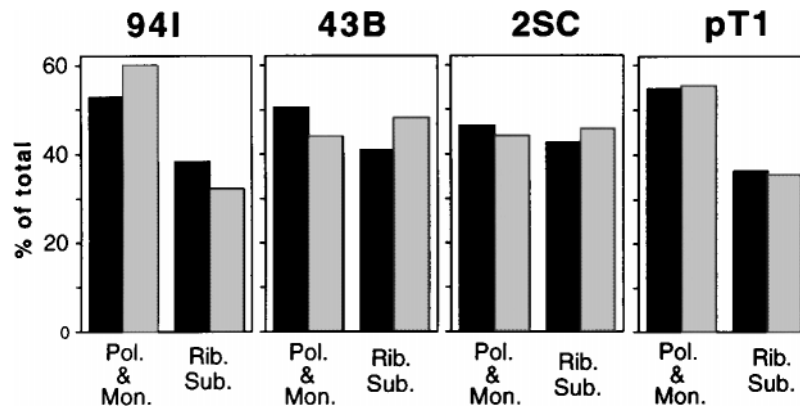


FIG. 8. Bar graph distribution of steady state levels of mitochondrial rRNAs in sucrose gradient fractions from mitochondrial lysates of 94I wild-type cells, 43B and 2SC MELAS mutant cells, and pT1 MERRF mutant cells. Mitochondrial lysates from the indicated cell lines were fractionated on sucrose gradients, and the RNA from every fraction and from the pellets was extracted. RNA gel blot analysis was carried out on the extracted RNAs, and the hybridization signals were quantified by PhosphorImager analysis. In all experiments, the amount of 16 and 12 S rRNAs migrating near the meniscus was $\leq 11\%$ of the total and is not shown. Pol. & Mon., polysomes and monosomes; Rib. Sub., ribosomal subunits. Black bars, 16 S rRNA; gray bars, 12 S rRNA.

mutant cells as well as in cells carrying the T3271C MELAS mutation (16). In light of the evidence that has been presented that post-transcriptional modifications of yeast tRNA^{ASP} can play a role in aminoacylation (42), it is possible that the undermodifications mentioned above contribute further to the reduced aminoacylation of the tRNA^{Leu(UUR)}.

Yasukawa *et al.* (16) have shown that the mutant tRNA^{Leu(UUR)} is aminoacylated with only leucine, thereby eliminating one possible route of misincorporation. The observations in the present work on the stability of mitochondrial proteins tend to rule out misincorporation by other routes as well.

Lack of Correlation between Individual Protein Synthesis Rates and UUR Codon Content of mRNA—Previous work from this laboratory has established that protein synthesis defects due to some tRNA mutations can be explained by logical models of elongation defects. Thus, in the case of the mitochondrial tRNA^{Lys} A8344G mutation associated with the MERRF encephalomyopathy, evidence for premature termination of translation (or premature dissociation of ribosomes) was provided by 1) the presence of truncated translation products, 2) the observation that polysomes were smaller than in control cells, and 3) the finding that the residual rate of synthesis of the individual polypeptides was an exponential function of the number of lysine codons, as would be expected for premature termination of translation (5). A description of an identical model for a translation defect in an *Escherichia coli* mutant had been previously published by Goldman (43), who predicted and showed evidence for the same dependence of synthesis rate on an exponential function of the number of codons for which the charged tRNA was limiting.

In another instance, that of the T7445C transition affecting the synthesis of tRNA^{Ser(UCN)}, evidence for the transient pause model was provided by the absence of prematurely terminated translation products and, especially, by the observation that the residual rate of synthesis of the individual polypeptides was not a function of the number of UCN codons but of the proportion of these codons. Strikingly, the only exception to this rule involved the ND6 polypeptide, whose lower than expected rate of synthesis was shown to be due to a significant specific decrease in its mRNA level, a decrease that resulted from the effect of the T7445C mutation on RNA processing.

In A3243G mutation-carrying cells, the protein synthesis data did not fit either of the models of elongation defect. The lack of dependence of residual protein synthesis on UUR codon content, discussed above, suggests that protein synthesis in

A3243G MELAS cells is limited by a mechanism operating mainly at some step other than elongation. Furthermore, a defect occurring primarily at the level of elongation that does not lead to premature translation termination would be expected to produce larger polysomes in mutant cells, rather than the observed smaller ones.

Evidence for Defective Polysome Formation—The mechanism by which protein synthesis is affected by the A3243G mutation in the present studies was suggested by the striking findings pointing to a decrease in ribosome loading onto mRNA in the mutant cell lines 43B and 2SC. This decrease in ribosome loading was indicated 1) by the shift in polysome size toward smaller polysomes (monosomes and disomes) in the absence of prematurely terminated translation products, 2) by the appreciable increase in proportion of 16 and 12 S rRNAs sedimenting with free ribosomal subunits, and 3) by the increase in proportion of ND1 mRNA sedimenting with free subunits in 2SC. In contrast, no evidence was obtained of a shift of the two rRNA species and of mRNA to the ribosomal subunit region of the sucrose gradient of a mitochondrial lysate from the A8344G tRNA^{Lys} gene mutation-carrying pT1 cells, which also exhibit smaller polysome size, but, in this case, as a result of premature translation termination.

A possible explanation for the observations listed above is that the rate of initiation of mitochondrial translation is slowed in MELAS mutant cells. One plausible mechanism to be considered for a defect in initiation and for defective polysome formation in mutant cells is that shown to occur in the cytosol of mammalian cells after amino acid starvation (44). Amino acid starvation produced by omission of an essential amino acid from the medium blocks initiation of protein synthesis by causing an increase in phosphorylated eIF-2 (45). Studies with tRNA synthetase mutants and with specific inhibitors of aminoacylation have shown that uncharged tRNA in the cytosol of mammalian cells can mediate the amino acid starvation effect, blocking the formation of initiation complexes (46, 47).

Another possible mechanism of defective polysome formation in A3243G mutation-carrying cells may involve an unidentified important role of tRNA^{Leu(UUR)} in initiation of translation. The evidence of heterogeneity in secondary modifications observed in tRNA^{Leu(UUR)} (15, 16) and in its electrophoretic mobility (33) is consistent with this tRNA having more than one function. The multiplicity of functions of this tRNA gene may account both for the large number of disease-causing mutations found in this gene (1) and for the variability in phenotype associated with the A3243G mutation (1). It is interesting that the

tRNA^{Leu(UUR)} is one of the most abundant mitochondrial tRNAs synthesized by the whole H strand transcription unit in human cells (29). Strikingly, it is even more abundant than mitochondrial tRNA^{Leu(CUN)}, synthesized by the same transcription unit, although the CUN codons are 6-fold more abundant than the UUR codons. There are many examples of tRNAs having functions other than the decoding of mRNA (48).

Finally, although there is evidence (33) that the 16 S rRNA in mutant cells is processed correctly at the 3'-end (*i.e.* at the end most likely to be affected by the A3243G mutation), one cannot exclude the possibility that alterations in secondary modifications of 16 S rRNA may affect the association of the large ribosomal subunit with the mRNA-small subunit complex.

It is clear that further work is needed to clarify the source of the defective association of mRNA with ribosomes detected in the present work in MELAS mutation-carrying cells and the mechanism whereby, in the more severely affected 43B cells, the mRNA not assembled in polysomes becomes degraded.

Nature of the RNA Sedimenting at ~25 S—The heterogeneously sized [³H]uridine-labeled structures, with a median sedimentation constant of ~25 S, in the sucrose gradients from 43B cells have been shown to contain an excess of mRNA, relative to the corresponding region of control gradients. This accumulation of mRNA in the 25 S region of the gradient correlates with the strong decrease in polysome size in 43B cells. These ~25 S structures may represent an RNA degradation complex similar to the 500-kDa degradosome that has been described in *E. coli* and functions in normal mRNA turnover (49). More recently, similar structures have been observed in yeast mitochondria, where they function in intron turnover (50), and in plastids, where they function in mRNA processing (51). It is conceivable that more mRNA enters RNA-degrading complexes in 43B mutant cells than in wild-type cells, because of the severe defect of association of mRNA with polysomes in this cell line.

Respiratory Phenotype Associated with the A3243G Mutation—2SC mutant cells exhibit only a moderate decrease in overall rate of mitochondrial protein synthesis (20–40%), yet they have a low rate of O₂ consumption, 0.86 fmol/min/cell, as compared with 4.7 fmol/min/cell in the corresponding wild-type transformant (2SA) (11). Low respiration rates or respiratory enzyme rates in A3243G mutation-carrying cybrids have been found by others as well (17, 18, 52). A plausible observation for this phenomenon is the finding in the present work of a marked decrease in the rate of synthesis of the ND6 subunit of NADH dehydrogenase (complex I), which is in agreement with the observations of Dunbar *et al.* (52). There is good evidence that this enzyme complex is rate-limiting for respiration (53, 54). In some MELAS patients (55–57), and also in A3243G mutant transmittochondrial cell lines (52), a disproportionate deficiency of complex I relative to the other respiratory complexes has been reported. Furthermore, it has been shown that the ND6 subunit is essential for the assembly and activity of complex I in mouse cells (58).

Proposed Model of Pathogenetic Mechanism—In summary, previously published work and the evidence presented here suggest the following model for the effects of the A3243G mutation on mitochondrial protein synthesis and respiratory chain function. The A3243G mutation causes an alteration in the tertiary structure of the tRNA^{Leu(UUR)}, a deficiency of methylation of the G at nucleotide 3239 (15), and a deficiency of modification of uridine at the first position of the anticodon (16). As a consequence of the tertiary structure alteration or of the reduced secondary modifications, or of both, the mutant tRNA^{Leu(UUR)} is metabolically less stable and is charged to a

lesser extent by the leucyl-tRNA synthetase. The reduced level of charged tRNA, or the reduced ratio of charged to uncharged tRNA, or some other as yet unknown factor related to the mutation then affects mRNA association with ribosomes, possibly through an effect on a mitochondrial translation initiation factor, like IF-2_{mt} (59), causing a general reduction in mitochondrial protein synthesis rate. In severely affected cells, the degradation of mRNAs not associated with ribosomes becomes apparent.

Acknowledgments—We thank Susan Lai, Shili Duan, Benneta Keeley, and Arger Drew for technical assistance.

REFERENCES

- Schon, E. A., Bonilla, E., and DiMauro, S. (1997) *J. Bioenerg. Biomembr.* **29**, 131–149
- Shoffner, J. M., Lott, M. T., Lezza, A. M. S., Seibel, P., Ballinger, S. W., and Wallace, D. C. (1990) *Cell* **61**, 931–937
- Reid, F. M., Vernham, G. A., and Jacobs, H. T. (1994) *Hum. Mutat.* **3**, 243–247
- Fischel-Ghodsian, N., Prezant, T. R., Fournier, P., Stewart, I. A., and Maw, M. (1995) *Am. J. Otolaryngol.* **16**, 403–408
- Enriquez, J. A., Chomyn, A., and Attardi, G. (1995) *Nat. Genet.* **10**, 47–55
- Guan, M.-X., Enriquez, J. A., Fischel-Ghodsian, N., Puranam, R. S., Lin, C. P., Maw, M. A., and Attardi, G. (1998) *Mol. Cell. Biol.* **18**, 5868–5879
- Goto, Y., Nonaka, I., and Horai, S. (1990) *Nature* **348**, 651–653
- van den Ouweland, J. M. W., Lemkes, H. H. P. J., Ruitenbeek, W., Sandkuijl, L. A., de Vijlder, M. F., Struyvenberg, P. A. A., van den Kamp, J. J. P., and Maassen, J. A. (1992) *Nat. Genet.* **1**, 368–371
- Johns, D. R., and Hurko, O. (1991) *Lancet* **337**, 927–928
- Kruse, B., Narasimhan, N., and Attardi, G. (1989) *Mol. Cell. Biol.* **58**, 391–397
- Chomyn, A., Martinuzzi, A., Yoneda, M., Daga, A., Hurko, O., Johns, D., Lai, S. T., Nonaka, I., Angelini, C., and Attardi, G. (1992) *Proc. Natl. Acad. Sci. U. S. A.* **89**, 4221–4225
- Hess, J. F., Parisi, M. A., Bennett, J. L., and Clayton, D. A. (1991) *Nature* **351**, 236–239
- King, M. P., Koga, Y., Davidson, M., and Schon, E. A. (1992) *Mol. Cell. Biol.* **12**, 480–490
- Schon, E. A., Koga, Y., Davidson, M., Moraes, C. T., and King, M. P. (1992) *Biochim. Biophys. Acta* **1101**, 206–209
- Helm, M., Florentz, C., Chomyn, A., and Attardi, G. (1999) *Nucleic Acids Res.* **27**, 756–763
- Yasukawa, T., Suzuki, T., Suzuki, T., Uedo, T., Ohta, S., and Watanabe, K. (2000) *J. Biol. Chem.* **275**, 4251–4257
- Flierl, A., Reichmann, H., and Seibel, P. (1997) *J. Biol. Chem.* **272**, 27189–27196
- Janssen, G. M. C., Maassen, J. A., and van den Ouweland, J. M. W. (1999) *J. Biol. Chem.* **274**, 29744–29748
- Chomyn, A., Meola, G., Bresolin, N., Lai, S. T., Scarlato, G., and Attardi, G. (1991) *Mol. Cell. Biol.* **11**, 2236–2244
- Yoneda, M., Chomyn, A., Martinuzzi, A., Hurko, O., and Attardi, G. (1992) *Proc. Natl. Acad. Sci. U. S. A.* **89**, 11164–11168
- King, M. P., and Attardi, G. (1989) *Science* **246**, 500–503
- Micol, V., Fernandez-Silva, P., and Attardi, G. (1997) *J. Biol. Chem.* **272**, 18896–18904
- Micol, V., Fernandez-Silva, P., and Attardi, G. (1996) *Methods Enzymol.* **264**, 3–11
- Maxam, A. M., and Gilbert, W. (1980) *Methods Enzymol.* **65**, 499–560
- Enriquez, J. A., and Attardi, G. (1996) *Methods Enzymol.* **264**, 183–196
- Varshney, U., Lee, C.-P., and RajBhandary, U. L. (1991) *J. Biol. Chem.* **266**, 24712–24718
- Chomyn, A. (1996) in *Methods Enzymol.* **264**, 197–211
- Ojala, D., and Attardi, G. (1972) *J. Mol. Biol.* **65**, 273–289
- King, M. P., and Attardi, G. (1993) *J. Biol. Chem.* **268**, 10228–10237
- Feinberg, A. P., and Vogelstein, B. (1984) *Anal. Biochem.* **137**, 266–267
- Anderson, S., Bankier, A. T., Barrell, B. G., de-Brujin, M. H. L., Coulson, A. R., Drouin, J., Eperon, I. C., Nierlich, D. P., Roe, B. A., Sanger, F., Schreier, H. P., Smith, A. J. H., Stader, R., and Young, I. G. (1981) *Nature* **290**, 427–465
- El Meziane, A., Lehtinen, S. K., Hance, N., Nijtmans, L. G. J., Dunbar, D., Holt, I. J., and Jacobs, H. T. (1998) *Nat. Genet.* **18**, 350–353
- Koga, Y., Davidson, M., Schon, E. A., and King, M. P. (1993) *Nucleic Acids Res.* **21**, 657–662
- O'Brien, T. W. (1971) *J. Biol. Chem.* **246**, 3409–3417
- Goddard, J. P. (1977) *Prog. Biophys. Mol. Biol.* **32**, 233–308
- Normanly, J., and Abelson, J. (1989) *Annu. Rev. Biochem.* **58**, 1029–1049
- Schimmel, P., Giegé, R., Moras, D., and Yokoyama, S. (1993) *Proc. Natl. Acad. Sci. U. S. A.* **90**, 8763–8768
- Saks, M. E., Sampson, J. R., and Abelson, J. N. (1994) *Science* **263**, 191–197
- Hou, Y. M., Westhof, E., and Giegé, R. (1993) *Proc. Natl. Acad. Sci. U. S. A.* **90**, 6776–6780
- Puglisi, J. D., Putz, J., Florentz, C., and Giegé, R. (1993) *Nucleic Acids Res.* **21**, 41–49
- Senger, B., and Fasiolo, F. (1996) *Biochimie (Paris)* **78**, 597–604
- Perret, V., Garcia, A., Grosjean, H., Ebel, J.-P., Florentz, C., and Giegé, R. (1990) *Nature* **344**, 787–789
- Goldman, E. (1982) *J. Mol. Biol.* **158**, 619–636
- Van Venrooij, W. J. W., Henshaw, E. C., and Hirsch, C. A. (1972) *Biochim. Biophys. Acta* **259**, 127–137
- Scorsone, K. A., Panniers, R., Rowlands, A. G., and Henshaw, E. C. (1987)

- J. Biol. Chem.* **262**, 14538–14543
46. Vaughan, M. H., and Hansen, B. S. (1973) *J. Biol. Chem.* **248**, 7087–7096
47. Austin, S. A., Pollard, J. W., Jagus, R., and Clemens, M. J. (1986) *Eur. J. Biochem.* **157**, 39–47
48. Söll, D. (1993) in *The RNA World* (Gesteland, R., and Atkins, J., eds) pp. 157–184, Cold Spring Harbor Laboratory, Cold Spring Harbor, NY
49. Py, B., Causton, H., Mudd, E. A., and Higgins, C. F. (1994) *Mol. Microbiol.* **14**, 717–729
50. Margossian, S. P., Li, H., Zassenhaus, H. P., and Butow, R. A. (1996) *Cell* **84**, 199–209
51. Hayes, R., Kudla, J., Schuster, G., Gabay, L., Maliga, P., and Grussem, W. (1996) *EMBO J.* **15**, 1132–1141
52. Dunbar, D. R., Moonie, P. A., Zeviani, M., and Holt, I. J. (1996) *Hum. Mol. Genet.* **5**, 123–129
53. Hofhaus, G., and Attardi, G. (1995) *Mol. Cell. Biol.* **15**, 964–974
54. Bai, Y., Shakeley, R. M., and Attardi, G. (2000) *Mol. Cell. Biol.* **20**, 805–815
55. Tanaka, M., Nishikimi, M., Suzuki, H., Ozawa, T., Nishizawa, M., Tanaka, K., and Miyatake, T. (1986) *Biochem. Biophys. Res. Commun.* **140**, 88–93
56. Kobayashi, M., Morishita, H., Sugiyama, N., Yokochi, K., Nakano, M., Wada, Y., Hotta, Y., Terauchi, A., and Nonaka, I. (1987) *J. Pediatr.* **110**, 223–227
57. Ichiki, T., Tanaka, M., Nishikimi, M., Suzuki, H., Ozawa, T., Kobayashi, M., and Wada, Y. (1988) *Ann. Neurol.* **23**, 287–294
58. Bai, Y., and Attardi, G. (1998) *EMBO J.* **17**, 4848–4858
59. Ma, L., and Spremulli, L. L. (1995) *J. Biol. Chem.* **270**, 1859–1865